

Experimental Investigation of a Morphing Nacelle Ducted Fan

Shayne A. Kondor

Georgia Tech Research Institute
Smyrna, GA

shayne.kondor@gtri.gatech.edu

Mark Moore

NASA Langley Research Center
Hampton, VA

mark.d.moore@nasa.gov

Abstract

The application of Circulation Control to the nacelle of a shrouded fan is proposed as a means to enhance off-design performance of the shrouded fan. Typically, a fixed geometry shroud is efficient at a single operating condition. Modifying circulation about the fixed geometry is proposed as a means to virtually *morph* the shroud without moving surfaces. This approach will enhance off-design-point performance with minimal complexity, weight, and cost. Termed the *Morphing Nacelle*, this concept provides an attractive propulsion option for Vertical Take-off and Landing (VTOL) aircraft, such conceptual Personal Air Vehicle (PAV) configurations proposed by NASA. An experimental proof of concept investigation of the *Morphing Nacelle* is detailed in this paper.

A powered model shrouded fan model was constructed with Circulation Control (CC) devices integrated in the inlet and exit of the nacelle. Both CC devices consisted of an annular jet slot directing a jet sheet tangent to a curved surface, generally described as a Coanda surface. The model shroud was tailored for axial flight, with a diffusing inlet, but was operated off-design condition as a static lifting fan. Thrust stand experiments were conducted to determine if the CC devices could effectively improve off-design performance of the shrouded fan. Additional tests were conducted to explore the effectiveness of the CC devices a means to reduce peak static pressure on the ground below a lifting fan.

Experimental results showed that off-design static thrust performance of the model was improved when the CC devices were employed under certain conditions. The exhaust CC device alone, while effective in diffusing the fan exhaust and improving weight flow into shroud inlet, tended to diminish performance of the fan with increased CC jet momentum. The inlet CC device was effective at reattaching a normally stalled inlet flow condition, proving an effective means of enhancing performance. A more dramatic improvement in static thrust was obtained when the inlet and exit CC devices were operated in unison, but only over a limited range of CC jet momentums. Operating the nacelle inlet and exit CC devices together proved very effective in reducing peak ground plane static pressure, while maintaining static thrust. The *Morphing Nacelle* concept proved effective at enhancing off-design performance of the model; however, additional investigation is necessary to generalize the results

Background

Fan and Shroud Interactions

The shrouded (or ducted) fan presents a solution for efficient powered lift and forward flight propulsion of Vertical Take-Off and Landing (VTOL) aircraft configurations. The geometry of the shroud has a significant effect on the efficiency of the fan (or propeller) due to the mutual interaction of the shroud and fan. Shroud geometry affects the velocity and pressure at the propeller plane, while maintaining a finite loading out at the tips of the fan blades¹. With proper design consideration, performance and efficiency of the shrouded fan will exceed the performance of a similar open propeller configuration operating in the same freestream condition. However, the geometry of a shroud designed for maximum static thrust will differ significantly from a shroud designed the peak efficiency in axial translation. The sense of circulation (Γ) about an optimal shroud design reverses as the operating condition changes from static thrust generation to high-speed axial flight.

Ideally, the shroud of a static (lifting) fan features a generous bell-mouth inlet converging toward the exit nozzle (see Figure 1). Flow entering the inlet is accelerated into the fan by the sense circulation about the shroud (depicted by the yellow arrows), resulting in an overall increase in thrust (compared to an open propeller operating under the same conditions)¹, and a significant lifting pressure difference on the shroud. Accelerating shroud designs generally possess a negative camber line and thicker crosssections. While these designs are efficient at producing static thrust, they suffer significant drag penalties in axial flight; thus, are ineffective for axial flight.

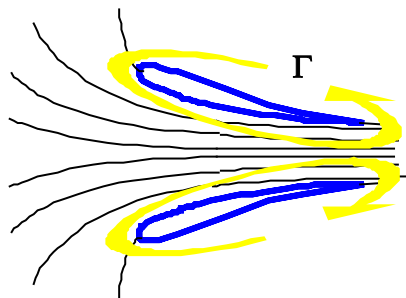


Figure 1.
Accelerating Shroud Circulation

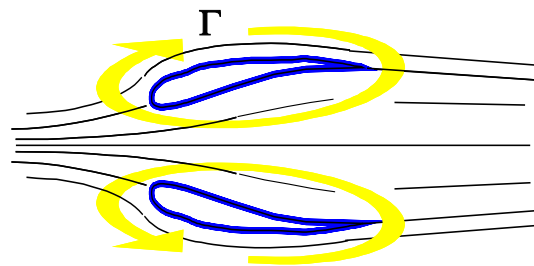


Figure 2.
Decelerating Shroud Circulation

Decelerating, or diffusing, shroud designs are generally employed for axial flight applications (see Figure 2). Decelerating shroud designs generally feature a positive camber line and a thin crosssection. In this case, circulation (Γ) on the shroud acts to decelerate the flow entering the inlet to below freestream speed. A net thrust is developed on the shroud as a result of the static pressure rise in the inlet, while the benefits of finite blade loading are realized at the propeller.

Proper shroud design for the intended operating condition will yield a net increase in performance over an open propeller of similar size.

The Morphing Nacelle Concept

The shroud geometries presented in Figures 1 & 2 are, of course, idealized cases where the camberline of the shroud is nearly a streamline in the flow. Neither design would work well in a real application that deviates from the ideal design conditions. However, a case can be made that actively modifying the circulation around the shroud may be a means to enhance effectiveness in off design operation. This can, of course, be achieved by complicated variable geometry inlets and nozzles, or alternately by applying means of circulation control to effectively *morph* a fixed geometry shroud.

The concept of modifying shroud circulation as a means to enhance propulsive performance was proposed by Morel & Lissaman² and investigated more recently by Heiges & Kondor³. The first approach sought to augment weight flow through the shrouded fan by injection of high momentum flow near the aft stagnation point of the shroud, effectively moving the upstream stagnation point, thus, affecting the entire flow field. Morel & Lissaman presented several theoretical models, treating the effect as a virtual diffuser at the fan exit; the shroud was treated as uncambered, vanishingly thin surface, with a pneumatic jet injected at an angle away from the exhaust at the shroud exit, similar to a jet flap. This jet was intended to entrain and turn the flow exhausting from the shroud, thus was termed a jet flap diffuser. The shroud and jet flap diffuser were modeled as a potential flow problem. This analysis predicted a net increase in static thrust and weight flow through the shroud, at a fixed power setting shared between the fan and the jet flap diffuser, and a propulsive efficiency gain due to an expanded wake stream tube. More recently, Heiges & Kondor developed a powered model to experimentally investigate the modification of circulation about a three dimensional shrouded fan as a means of generating control forces and moments. In the latter case, a tangent wall jet was directed over a curved surface at the shroud exit to form a Coanda surface, as shown in Figure 3. This approach was adapted from proven means of circulation control on wings⁴, and wrapped around the exit of an axisymmetric fan shroud. Tuft visualizations showed the approach to be effective in turning the efflux from the model, as well as generating significant sideforce when applied over a limited sector of the shroud exit.

Investigators in the NASA Personal Air Vehicle (PAV) program proposed the application of circulation control to a fixed geometry shroud as a means to optimize performance across a variety of flight conditions, without the weight penalty of variable geometry inlets and nozzles. This fan shroud concept was dubbed the *Circulation Control Morphing Nacelle*. In support of the PAV investigation, Georgia Tech Research Institute (GTRI) and M-Dot Aerospace developed a powered model shrouded fan with a *Circulation Control Morphing Nacelle*. Reconfigurable CC jet devices were integrated into the fan shroud inlet and nozzle exit, allowing for a variety of Morphing Nacelle approaches to be

investigated. The model was installed in the Model Test Facility thrust cell at Georgia Tech Research Institute in October 2002, and has been used in investigations of the morphing nacelle concept up to the present.

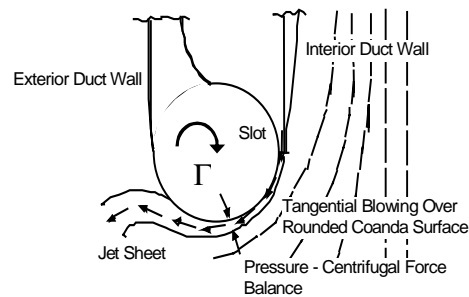


Figure 3. Section View Circulation Control Device Integrated at the Exit of an Axisymmetric Duct (adapted from Englar⁴).

Circulation Control Aerodynamics

The aerodynamic concept now known as Circulation Control (Figure 3 & Reference 4) is a means to directly enhance aerodynamic/hydrodynamic forces generated on a body of fixed geometry. The concept employs the injection of momentum into the flow field over a body in a manner that affects the entire flow field. As explained by Englar⁴ for a lifting body:

[typically] a tangential jet sheet exits over the curved trailing edge of the surface [often replacing a flap or control surface], and this curvature can turn through a full 180° or more. The jet remains attached to that curved surface because of a balance between the sub-ambient pressure in the jet sheet and the centrifugal force around the curvature. Initially, at very low blowing values, the jet entrains the boundary layer to prevent aft flow separation, and is thus a very effective boundary layer control (BLC). Eventually, as the jet continues to turn, a rise in the static pressure plus viscous shear stress and centrifugal force combine to separate the jet sheet, and a new stagnation point and streamline are formed on the lower surface. The large flow entrainment rate of the jet and the large deflection of the stagnation streamline produce a pneumatic camber, and thus pneumatic control of the airfoil's circulation and lift. Although it is a very effective BLC, the interest in this device comes from its ability to further augment the circulation and lift, and thus the name Circulation Control (CC).

Historically, the use of a jet over a segmented curved surface to entrain flow is attributed to Henri Coanda, and is often referred to as the *Coanda Effect*⁴. The curved, or turning surface, is similarly referred to as a *Coanda surface*.

The cost of affecting a change in circulation is generally related in terms of a ratio of the CC jet momentum to the momentum of the flow being affected. Mass flow (\dot{m}_{jet}) and jet speed (V_{jet}) are captured in a non-dimensional

Momentum Coefficient:
$$C_{\mu} = \frac{\dot{m}_{jet} V_{jet}}{QS} \quad (\text{eq. 1}),$$

where Q is the freestream dynamic pressure and S a reference area. It is obvious that this standard expression for C_{μ} is not suitable for a static application with zero freestream dynamic pressure. Therefore, a new static C_{μ} term was defined for static, propulsive applications such as the CC Morphing Nacelle⁵. The new nondimensional term is based on fan angular speed (N) and diameter (D) in the typical manner used to nondimensionalize propeller thrust as a Thrust

Coefficient C_{ts} ⁶:
$$C_{ts} = \frac{Thrust}{\rho_{\infty} N^2 D^4} \quad (\text{eq. 2}).$$

This definition of C_{ts} captures ambient conditions and the key fan design variables affecting the power required to impart a momentum change to the flow. Using the same denominator terms as eq. 2, a *static momentum coefficient*, $C_{\mu s}$,

is defined, similar to eq. 1 :
$$C_{\mu s} = \frac{\dot{m}_{jet} V_{jet}}{\rho_{\infty} N^2 D^4} \quad (\text{eq. 3}).$$

The ratio of $C_{\mu s}/C_t$ provides a metric of the relative power requirement for the CC jet compared to the fan.

Experimental Investigation

Experimental investigations of the CC Morphing Nacelle were conducted using a powered model fan with tangent jet devices integrated into the inlet and exhaust of the nacelle. The objective of the experimental investigation was to determine the effectiveness of Circulation Control as a means of enhancing off-design operation of a shrouded fan with fixed nacelle geometry. A shrouded fan designed for high speed axial flight (similar to the configuration in Figure 2) was tested in static operation as a free jet and in proximity of a ground plane (in order to simulate lifting fan operation). Combinations of CC jet parameters were tested to modify circulation at inlet and exhaust of the nacelle, in the sense depicted in Figure 1. Simultaneous measurements of aggregate thrust, nacelle weight flow (\dot{m}_g), and ground plane pressure profile were made at a variety of CC jet strengths - while operating a fixed fan speed.

Figure 4 depicts the powered CC Morphing Nacelle model in crosssection. The powered fan core is depicted, along with the integral CC jet devices. The curved arrows at the nacelle inlet and exit depict jet sheet direction, and sense of added circulation.

The powered model was based on a Tech Development Inc., Model 457 pneumatic tip drive fan. The fan core consisted of a single stage turbine with 16

fixed pitch blades, on a shaft supported by fixed pitch stators. High pressure air was exhausted over a segregated outer ring of turbine blades to power the fan core; drive air exhausted through the power turbine mixed with the fan core flow before exiting the nacelle. Pressure ratios up to 1.20 were feasible, operating the fan up to 35,000 RPM.

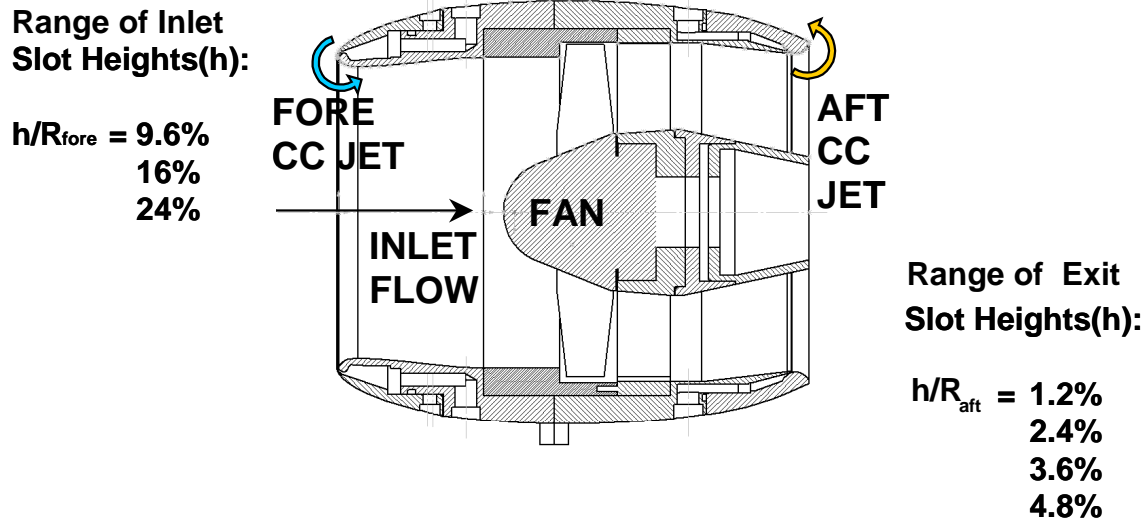


Figure 4. Section View of the Morphing Circulation Control Model

The nacelle design featured a decelerating inlet and parallel exhaust nozzle, providing a nacelle section camber similar to the decelerating shroud design depicted in Figure 2. A tangent jet slot was integrated at the leading edge of the nacelle section, intended to accelerate a jet around the maximum curvature of the inlet (the inlet wall acting as the Coanda surface). The inner and outer surfaces of the nacelle inlet were configured as concentric sections. The outer surface section could be positioned axially (along the fan centerline) to set the CC jet slot height; jet slot height (h) to inlet radius (R_{fore}) ratios could be varied from 9.6% to 24%. Similarly, a tangent jet slot was placed at the nacelle exit to generate a *virtual* diffuser effect. The jet sheet was directed over a quarter-round ring concentric to the nacelle exit. The curved surface formed by the ring was intended to act as a Coanda surface, promoting diffusion of the fan exhaust by low pressure generated over the surface. Interchangeable diffuser rings allowed for variations in CC jet slot height (h/R_{aft}) from 1.2%-4.8%, as indicated in Figure 4. The exit Coanda surface radius was double the inlet radius, accounting the difference in nondimensional slot heights.

Variations in CC jet slot height were tested in the steps listed in Figure 4. Likewise, jet momentum coefficient $C_{\mu S}$ was varied from zero up to values where fan performance was significantly diminished. The test matrix consisted of the permutations of jet slot configurations, tested over a range of $C_{\mu S}$ values for the inlet and exit jets, alone and in combination.

The powered fan model fan model (shown in the photo, Figure 5) was installed in the GTRI Model Test Facility Thrust Cell (as shown in Figure 6). The model was centered in the live, instrumented section of the thrust cell, providing

real time thrust measurement by electric load cells. Pneumatic supply lines were fed into the live balance frame (yellow frame in the photo, Figure 6) from a trapeze in order to minimize tear effects on thrust readings. Piloted pressure regulators mounted to the live balance controlled CC jet weight flow. Critical flow nozzles were placed downstream of the regulators to meter weight flow through the CC jet slots, also serving prevent communication between the fore and aft jet slots through the supply lines.

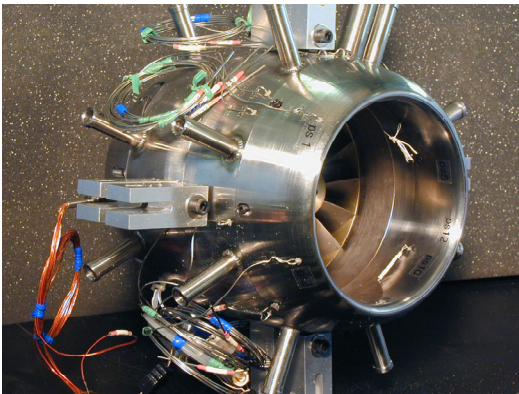


Figure 5. Powered Fan Model



Figure 6. Thrust Cell Installation

Regulating air weight flow to the outer ring of the turbine controlled fan speed; drive air pressure was regulated by feedback control to maintain constant speed.

Angular speed sensors on the fan shaft and total pressure probes downstream of the stators determined fan operating conditions. Pressure ratio (PR) was determined as the ratio of the total pressure behind the fan to ambient total pressure. Total pressure behind the fan was determined by averaging the samples from a five probe total pressure rake located immediately downstream of the stator vanes.

Jet speed at each CC jet slot (V_j) was estimated from measurements of slot plenum stagnation conditions and discharge static pressure. The jet was assumed to function as an ideal isentropic converging nozzle discharging into the nacelle flow, following the relation:

$$V_j = \sqrt{2RT_d \left(\frac{\gamma}{\gamma-1} \right) \left[1 - \frac{P_\infty}{P_d} \right]^{\left(\frac{\gamma-1}{\gamma} \right)}} \quad (\text{eq. 4})$$

Where R is the gas constant, and γ the ratio of specific heats for air; P_d and T_d are the stagnation pressure and temperature in the jet slot supply plenum. According to Englar⁷, it is accepted practice in the application of Circulation Control to assume that the flow is discharging from the nozzle to freestream static pressure P_∞ . However, in static operation, the freestream assumption does not properly capture the discharge conditions into the nacelle flow, at either the

inlet or exit jet slot. Thus, static pressures were sampled in the internal nacelle flow to determine discharge conditions at the inlet (fore) jet slot and just upstream of the exit (aft) jet slot.

Experimental Results

Baseline Ducted Fan Performance

Baseline performance of the shrouded fan model was established by operating the fan as a free jet, out of ground effect (OGE), without CC slot weight flow. This mode of operation established the baseline performance across the operational range of fan pressure ratios (PR). Thrust was measured as fan drive air momentum (thus input power) was varied. When thrust data was nondimensionalized to a *Static Thrust Coefficient* C_{ts} (ref. eq. 2), the fan and nacelle combination was found to have a consistent baseline $C_{ts} = 0.068$ over an operating range of $1.05 < PR < 1.15$ (ref. Figure 7). The relationship of fan speed to pressure ratio was essentially linear over the same range of PR , and was directly related to drive air momentum (input power).

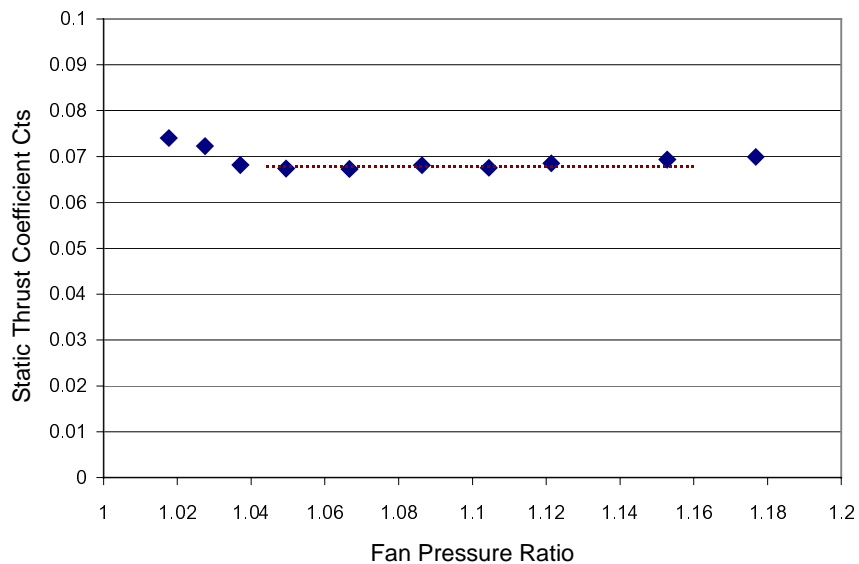


Figure 7. Static Thrust Performance of Baseline Fan-Nacelle Installation

Performance of the CC Morphing Nacelle – Free Jet

Nacelle Exit Circulation Control

The *Morphing Nacelle* was first tested in a free jet condition, the ground plane was removed from the thrust cell to provide an unobstructed path for the

fan's exhaust wake. An operating condition of $PR=1.10$ was selected as the starting point for sweeps of fore and aft CC jet momentum (values of $C_{\mu s}$).

Static operation tests were first conducted with only the exhaust CC jet active, sweeping jet strength over a range of $0 \leq C_{\mu s \text{ aft}} \leq 0.008$. Four jet slot heights were employed for this set of tests, as illustrated in Figure 4, while the turning surface radius and angle remained constant. The effect of applying CC at the fan exit proved to have a detrimental effect on overall static thrust performance, as shown in Figure 8. Modest gains in C_{ts} were obtained at values of $C_{\mu s \text{ aft}} < 0.002$, and only with the smaller jet gap heights h/R_{aft} of 1.2% and 2.4%. With increased CC jet momentum, $C_{\mu s \text{ aft}} > 0.002$, C_{ts} was generally diminished; little influence of jet slot height was noted. The weight flow into the nacelle inlet is shown in Figure 9. Weight flow was noted to rise with increasing $C_{\mu s \text{ aft}}$ up to $C_{\mu s \text{ aft}} = 0.004$, beyond which weight flow remained essentially constant. The increased weight flow indicated an increase in circulation in the sense depicted in Figure 1. An improvement in fan thrust would be expected with the increased weight flow into the nacelle inlet; however, it is thought that suction generated on the exit Coanda surface acted to reduce the overall thrust. A slight deficit in inlet weight flow is noted where the larger jet slot heights (3.6% & 4.8%) are employed. This weight flow deficit indicates that the thicker, slower jet sheets are not as effective at changing nacelle circulation as the faster thinner jet sheets.

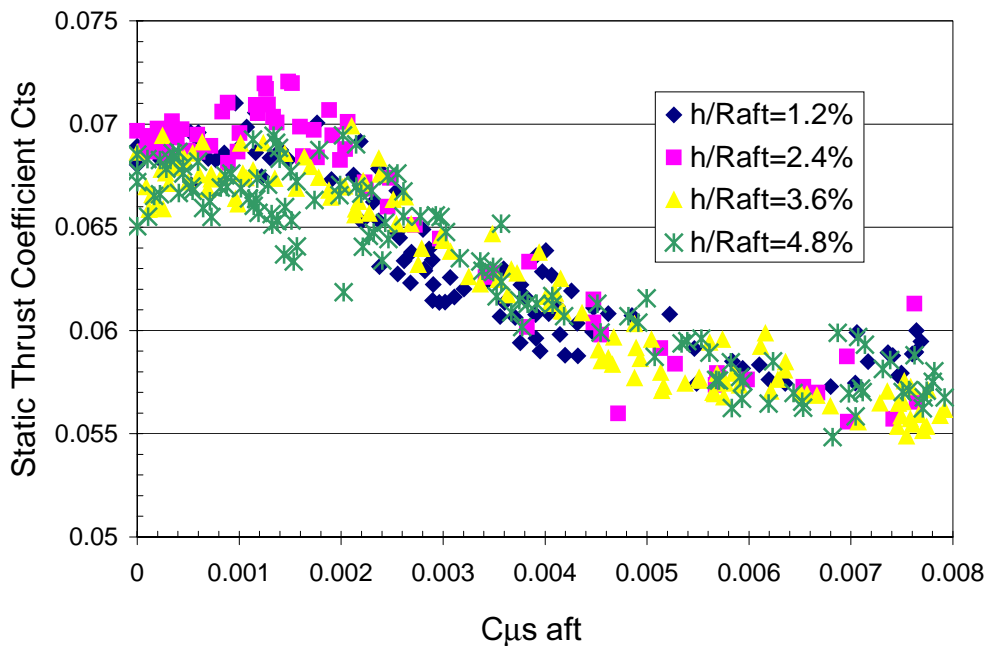


Figure 8. Static Thrust Performance with Exhaust CC Jet Active
Fan Speed 25 KRPM

Due to a lack of pressure instrumentation on the exit Coanda surface, the degree to which suction on the Coanda surface reduces the overall thrust could not be determined.

The measured fan pressure ratio remained essentially constant with variation of $C_{\mu s \text{ aft}}$, indicating that flow through the fan and stators was not detrimentally affected by the exit CC jet. Moreover, the fan speed, and fan input power setting, remained nearly constant over the range of $C_{\mu s \text{ aft}}$. Slight variations in fan speed and pressure ratio, from test point to test point, were accounted for by the nondimensional presentation of thrust as C_{ts} .

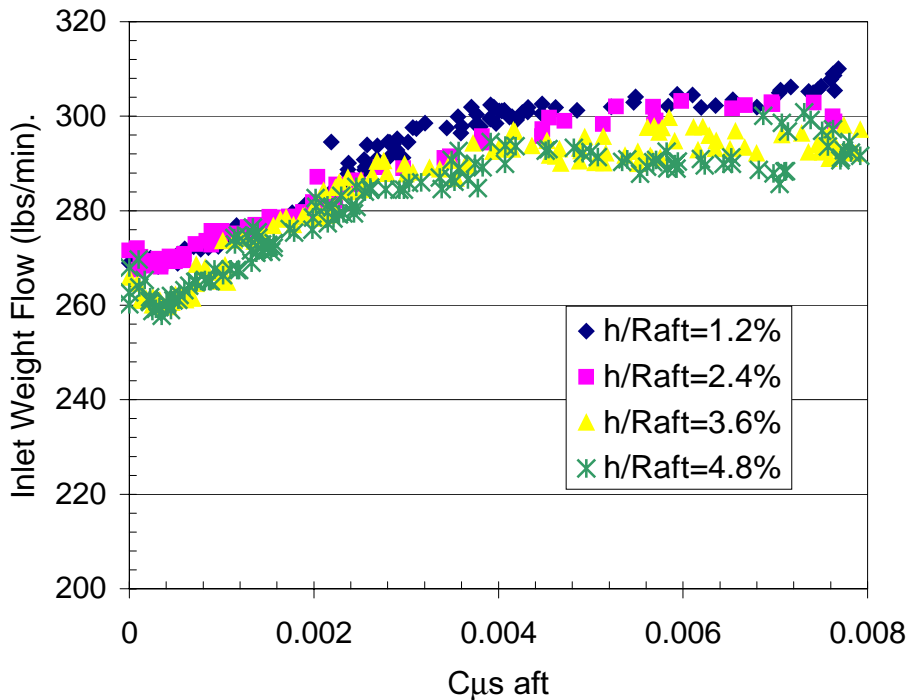


Figure 9. Nacelle Inlet Weight Flow with Exhaust CC Jet Active
Fan Speed 25 KRPM

The effect of the exit CC device on the fan efflux was explored with tuft grid visualization. The photographs in Figure 10 a, b, & c show the jet efflux from the nacelle exit at three values of $C_{\mu s \text{ aft}}$ (a false color image is presented to enhance contrast of the flow and tuft grid against the background). Tufts were placed in streamwise intervals of 1/2 of the nacelle exit diameter. The first case is the baseline jet with no CC active, showing a wake with a clear potential core, and little spreading is evident out to 3 diameters. The second and third cases reveal the effect of increasing the value of $C_{\mu s \text{ aft}}$. The application of the exit CC jet promotes a rapid spreading of the wake, and increased mixing. At very high jet strength, shown in Figure 10c, the potential core is lost by 1 dia. from the nacelle exit. This effect on the fan efflux indicates that a strong suction is generated on the Coanda surface.

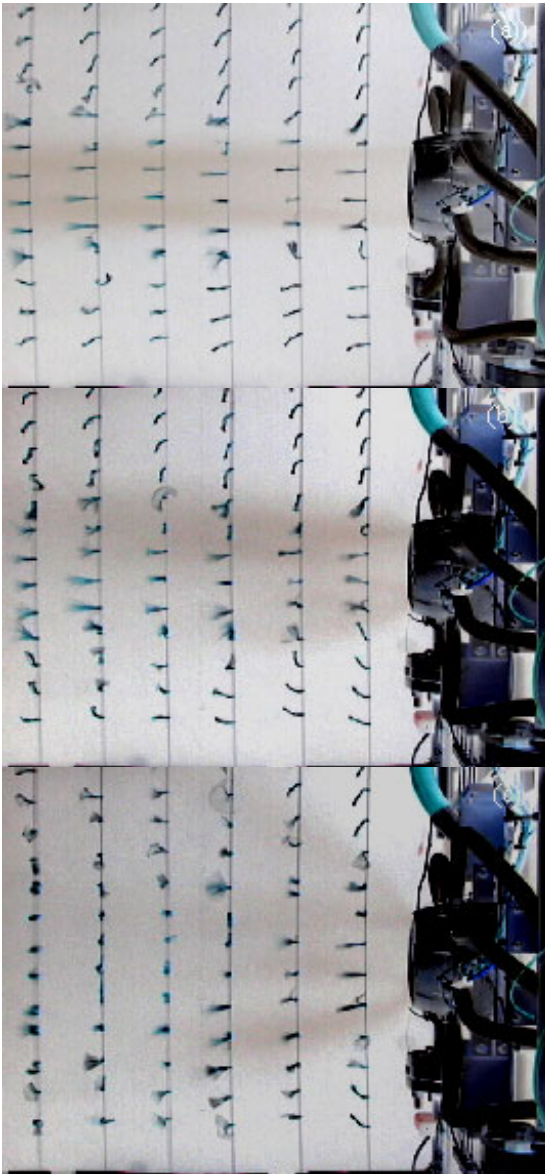


Figure 10 (a).

Fan Exhaust Flow Visualization with $C_{\mu s \text{ aft}} = 0$

Figure 10 (b).

Fan Exhaust Flow Visualization with $C_{\mu s \text{ aft}} = 0.007$

Figure 10 (a).

Fan Exhaust Flow Visualization with $C_{\mu s \text{ aft}} > 0.007$

Nacelle Inlet Circulation Control

The next series of test points investigated the effect of applying CC at the nacelle inlet. Three inlet CC jet slot heights were tested, as detailed in figure 4. Indicated fan pressure ration (PR) was found to vary as $C_{\mu s \text{ fore}}$ varied, indicating a change in fan operating condition with $C_{\mu s \text{ fore}}$. Holding constant fan PR would have required constant changes in fan power input and speed. However, the fan speed remained essentially constant at a constant power setting, despite increasing jet strength; thus, it was elected to hold fan speed constant during sweeps of $C_{\mu s \text{ fore}}$.

The variation of C_{ts} with $C_{\mu s \text{ fore}}$ is presented in Figure 11. A strong coupling was noted between the jet slot height and peak improvement in static thrust (C_{ts}); the smallest jet slot opening generally produced the maximum increase in static thrust for a given value of $C_{\mu s \text{ fore}}$. A peak gain of nearly 30% in

C_{ts} , over the baseline values, was obtained with the smallest slot height ($h/R_{fore} = 9.6\%$) at $C_{\mu\text{ fore}} = 0.004$. At this slot height C_{ts} abruptly dropped once $C_{\mu\text{ fore}}$ increased beyond 0.006, indicating an abrupt change in inlet flow conditions, possibly a forced separation of inlet flow.

For any value of $C_{\mu\text{ fore}}$ jet speed over the Coanda surface is greater using a smaller slot. The faster jet will generate a lower pressure over the Coanda surface, but may not remain attached around the sharp curvature of the nacelle's inlet. Slower, thicker jet sheets associated with the larger jet gaps will generate less suction on the leading edge, explaining the reduced performance noted with the larger jet slots. However these jets can remain attached at higher $C_{\mu\text{ fore}}$, alleviating the abrupt drop in performance note with the smallest jet slot.

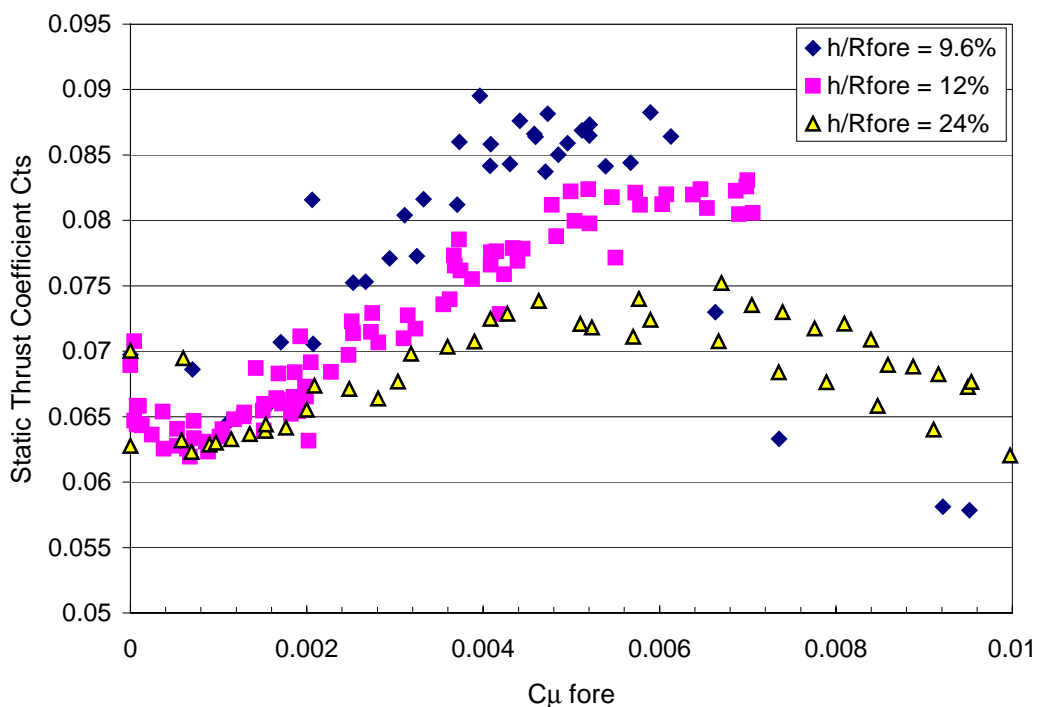


Figure 11. Static Thrust Performance with Inlet CC Jet Active

Improvements in C_{ts} for $C_{\mu\text{ fore}} > 0.002$ may be attributed to two sources: attachment of separated flow in the inlet, and suction generated in about the inlet lip (Coanda) surface by the acceleration of the jet around the inlet radius. An initial dip in C_{ts} is noted in the range of $0 < C_{\mu\text{ fore}} < 0.002$, for all slot heights. In this range inlet flow is separated, as shown by the tuft and oil flow visualizations in Figure 12 a. As $C_{\mu\text{ fore}}$ is increased the inlet flow attaches and C_{ts} subsequently rises, as does the inlet weight flow (ref. Figure 14). The attached inlet condition, with the inlet CC jet active, is shown in Figure 12 b.



Figure 12 (a). Inlet Flow $C_{\mu s \text{ fore}} = 0$



Figure 12 (b). Inlet Flow $C_{\mu s \text{ fore}} = 0.004$

Pressure instrumentation around the nacelle inlet was insufficient to verify the degree to which increased suction in the inlet contributed to the static thrust gains.

Combinations of Inlet and Exhaust Circulation Control

Simultaneous operation of the inlet and exit CC jets was the final free jet case tested. For these test runs, $C_{\mu s \text{ aft}}$ was held constant while $C_{\mu s \text{ fore}}$ was swept, and the full range of slot heights were tested. It was elected to hold fan speed constant while combinations of $C_{\mu s \text{ fore}}$ & $C_{\mu s \text{ aft}}$ were tested. Figure 13 presents the static thrust performance for a single slot height configuration.

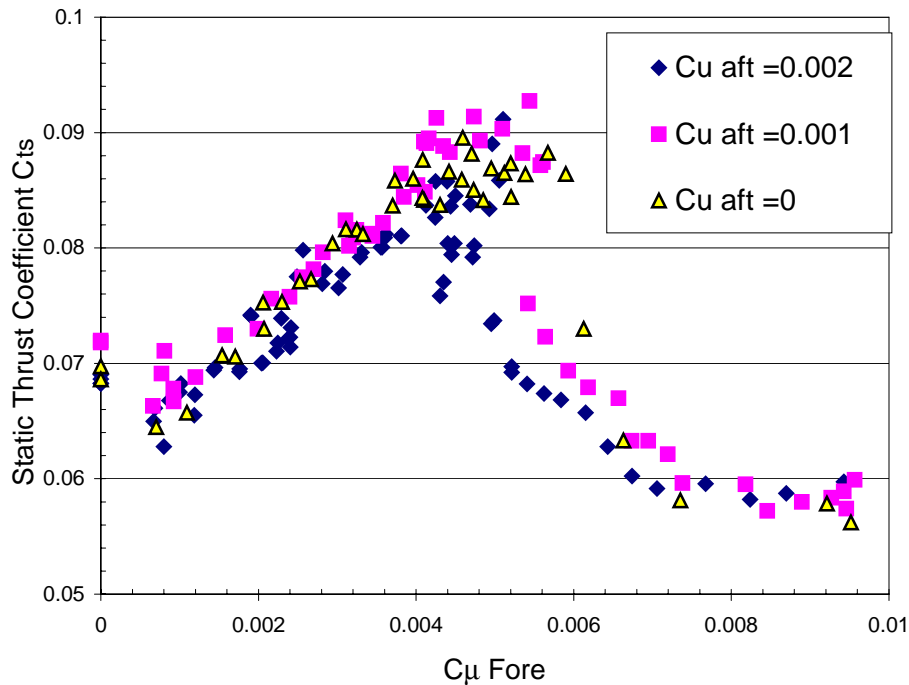


Figure 13. Static Thrust Performance with Combined Inlet and Exit CC
Fan Speed 25 KRPM, $h/R_{\text{fore}} = 9.6\%$, $h/R_{\text{aft}} = 2.4\%$

Comparing combined inlet and exit CC to the case of inlet CC only, a net gain in static thrust is noted with the application of the exit CC jet at small values ($C_{\mu \text{ aft}} = 0.001$). However, the performance is lost as $C_{\mu \text{ aft}}$ is increased (to $C_{\mu \text{ aft}} = 0.002$). In addition, the loss of thrust is greater when $C_{\mu \text{ fore}}$ is increased beyond to the value where inlet flow is forced to separate (the discontinuity occurring around $C_{\mu \text{ fore}} = 0.0055$). The characteristic response of the static thrust to increased $C_{\mu \text{ fore}}$ follows the same general trend whether $C_{\mu \text{ aft}}$ is active or inactive, indicating that the effect on inlet attachment is weakly coupled to the exit CC jet.

Increased static thrust performance at the lower value of $C_{\mu \text{ aft}}$ can be partially attributed to the increased weight flow generated by activation of the exit jet. Figure 14 illustrates an upward offset in weight flow when both CC devices are active (inlet CC jet weight flow was subtracted from the data). However, the increase in weight flow is still limited by flow condition in the inlet, abruptly dropping beyond the value of $C_{\mu \text{ fore}}$ where inlet flow is forced to separate.

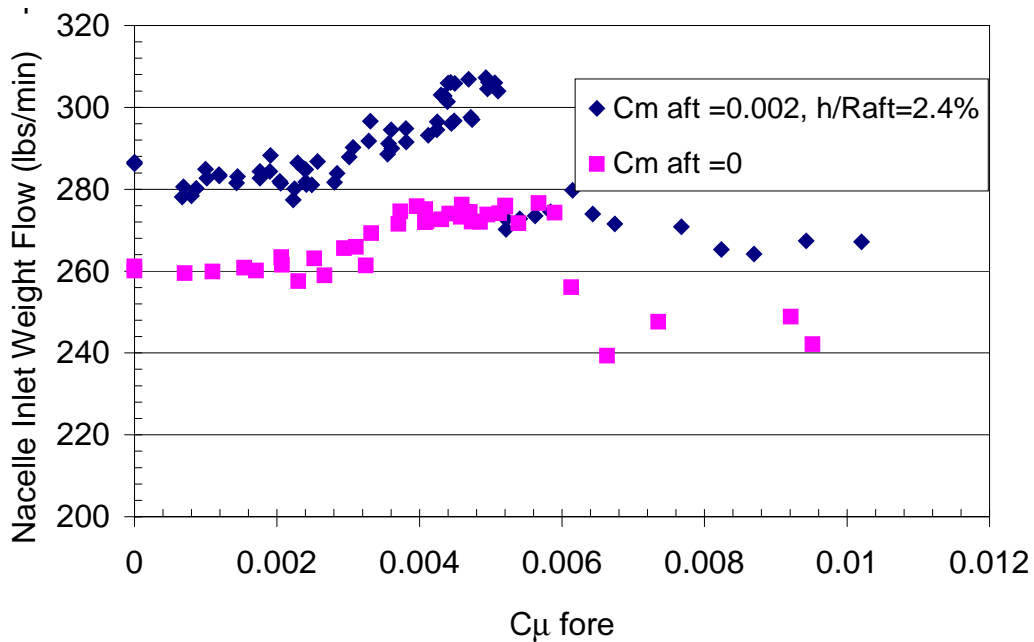


Figure 14. Nacelle Inlet Weight Flow with Inlet CC Active

Performance of the CC Morphing Nacelle – Hovering In Ground Effect

An instrumented ground plane was placed at set distances from the behind the fan exit in order to simulate hover in ground effect. The fan centerline was oriented normal to the ground plane, and in line with the central pressure tap. Ground plane static pressure taps were monitored to determine pressure at radial distances from the fan centerline.

Figure 15 presents a typical ground plane radial pressure profile, comparing cases of equivalent total thrust, with and without CC jets active.

Combinations of CC jet momentums were applied to achieve an equivalent thrust to the baseline case. As $C_{\mu s \text{ fore}}$ and $C_{\mu s \text{ aft}}$ were simultaneously increased, the peak pressure of the impinging wake was steadily reduced. Pressures inboard of 2.2 exit radii generally decreased, while outboard pressure increased (note these are radial stations and do not reflect equal ground plane areas), showing that fan momentum was retained as the wake spread over the ground.

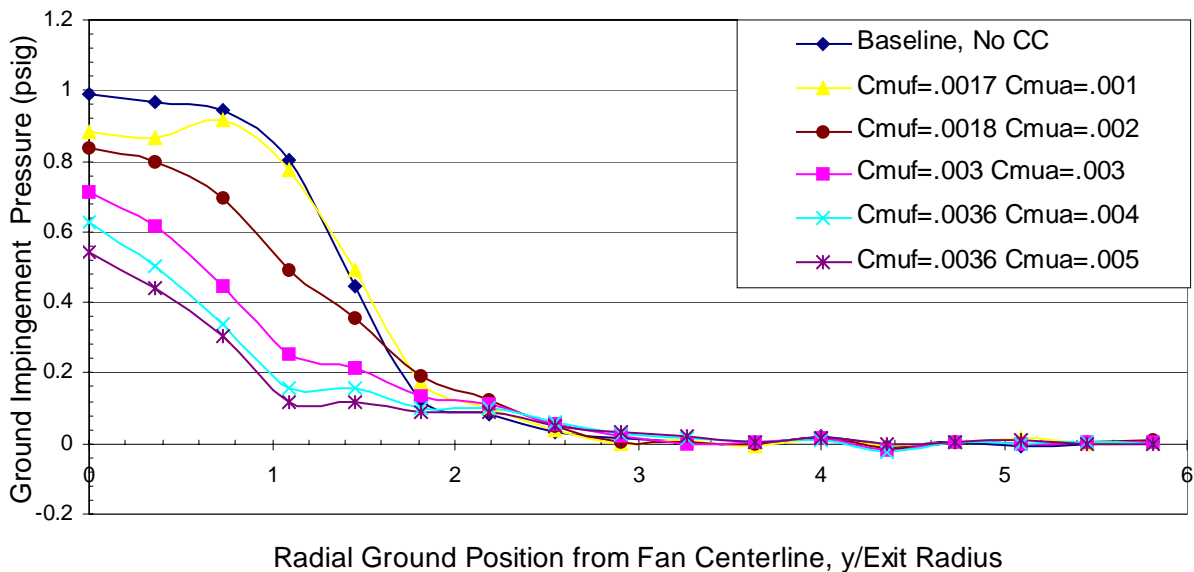


Figure 15. Ground Plane Static Pressure at 3 Exit Diameters Below the Fan
Fan Speed 25 KRPM, $h/R_{\text{fore}}=24\%$, $h/R_{\text{aft}}=4.8\%$, Thrust=44lbs ($C_t \sim 0.068$)

From the CC jet momentums listed in the legend of Figure 15, it is evident that increasing $C_{\mu s \text{ aft}}$ reduces the peak ground plane static pressure below the fan. This effect can be attributed to fan wake spreading and mixing generated by the exit CC jet (Ref. Figures 10 b & c). As $C_{\mu s \text{ aft}}$ was increased $C_{\mu s \text{ fore}}$ was likewise increased in order to maintain equivalent thrust to the baseline case. In this case suction on inlet surface may have balanced suction on the exhaust nozzle Coanda surface. It should be noted that the case presented in Figure 15 not an optimal case, it is based on maintaining constant thrust by CC jet changing CC jet parameters alone; equivalent thrust could be generated with optimal combinations of CC jet momentum at lower overall power settings.

Conclusions

Experimental results show that pneumatic jets directed over curved surfaces at the inlet and exit of the model shrouded fan nacelle improved static thrust under certain conditions. Increased weight flow through the nacelle inlet indicated that circulation about the shroud was increased by sufficient CC jet(s) momentum. The most notable improvement in static thrust coefficient was obtained when CC jet momentum was added at the nacelle inlet. CC jet

momentum applied at the exit proved far less effective in increasing static thrust, but did prove effective in reducing peak pressure impinging on the ground in simulated hover. A combination of inlet and exit CC momentum proved to be the most effective means to improve off-design performance of the shrouded fan.

Oil flow visualization showed the inlet CC jet to act as a separation control device. The diffusing inlet design, optimal for axial flight, suffered from inlet stall in static operation. The CC jet was effective in establishing flow attachment in the inlet, once sufficient momentum was injected into the flow. Improvement in static thrust performance was attributed to the improved inlet flow condition and suction generated on the nacelle's leading edge by the CC jet; however, inlet weight flow was only modestly improved indicating a small increase in circulation. The maximum performance gain was obtained with the smallest ratio of inlet jet slot height to turning radius tested: $h/R_{fore} = 9.6\%$; however, effectiveness was limited by the ability of the inlet flow to remain attached as CC jet momentum increased.

The nacelle exit CC device proved less effective in increasing static thrust, although more effective in increasing shroud circulation. Tuft flow visualization showed the exhaust flow stream tube was expanded by the exit CC device (as predicted by Lissaman for the *Jet Flap Diffuser*). An effective increase in shroud circulation was evident by the increased weight flow through the nacelle inlet. However, the only modest gains in net static thrust were obtained at very low jet momentum ($C_{\mu s aft}$), and static thrust was diminished as the jet momentum increased. The rise in inlet weight flow and drop in static thrust, seemingly contradictory observations, could be explained by considering the pressure drop generated on the Coanda surface at the nacelle's exit. Suction over the quarter round surface provides a significant component of force opposite of the static thrust vector. This is suspected as the cause of the loss in static thrust; however, instrumentation was not available to prove this hypothesis.

Maximum static performance gains were realized when the inlet and exit CC devices were operated together. Modest values of exit CC jet momentum ($C_{\mu s aft}$) further enhanced static thrust and nacelle inlet weight flow; however, the gains were limited inlet flow separation at high $C_{\mu s fore}$.

The combination of inlet and exit CC devices proved effective as a means to reduce ground plane static pressure under the fan. In comparison to the baseline operation of the shrouded fan in hover, nearly a 50% reduction in peak ground plane static pressure was observed when the CC jets were operated. This reduction in peak ground plane pressure was obtained without loss in static thrust, showing the morphing nacelle concept to be a viable means to reduce ground erosion by VTOL aircraft operation.

Recommendations

Further investigation of the application of circulation control on a shrouded fan nacelle, or *Morphing Nacelle*, is warranted. The results obtained in this study are insufficient to generalize the results for application to other shrouded fan configurations. The following additional studies are recommended:

- Continued investigation in static operation with pressure taps arrayed about the nacelle, particularly within the nacelle inlet and the over nacelle exhaust nozzle Coanda surface.
- Parametric study of exit Coanda surface turning angles to determine if static thrust can be enhanced by eliminating suction generated forces opposing the thrust vector.
- Development of a computational model, based on these experimental results, allowing for parametric studies of fan and shroud design variables.
- Investigation of unsteady CC jets as a means to reduce jet momentum requirements.

Acknowledgements

The experimental study detailed in this paper was supported by NASA Langley Research Center under contracts NAG-1-02093 and NAG-1-03055.

The authors wish to acknowledge the following individuals and organizations:

- Malik Little of GTRI , for many hours at the console completing the test matrix.
- Warren Lee of GTRI, for developing and supporting the data acquisition software.
- Bob Englar of GTRI, for insight in to the implementation of circulation control on the model.
- Frank Holman, Bryan Seegers, Hugh Spilsbury, and Scott Ashley, of M-Dot Aerospace; for the detail design and manufacture of the model.
- Sandy Shapery, of Shapery Gyronautics, for providing partial financial support for the fabrication of the model and lease of the TDI Fan core.

References

1. McCormick, B., *Aerodynamics of V/STOL Flight*, Academic Press 1967.
2. Morel, J., Lissaman P., *The Jet Flap Diffuser: A New Thrust Augmenting Device*; AIAA Paper 69-777, July 1969.
3. Kondor S., Heiges, M., *Active Flow Control for Control of Ducted Rotor Systems*, AIAA Paper 2001-0117, Jan. 2001.
4. Englar, R. J., *Circulation Control Pneumatic Aerodynamics: Blown Force and Moment Augmentation and Modification; Past, Present & Future*, AIAA Paper 2000-2541.
5. Kondor, et al., *Experimental Investigation of Circulation Control on a Shrouded Fan*, AIAA Paper 2003-3409
6. Perkins & Hage, *Airplane Performance, Stability, and Control*, Wiley, 1949

Experimental Investigation of Morphing Nacelle Ducted Fan

Shayne A. Kondor
Georgia Tech Research Institute
Smyrna, GA

Mark Moore
NASA Langley Research Center
Hampton, VA

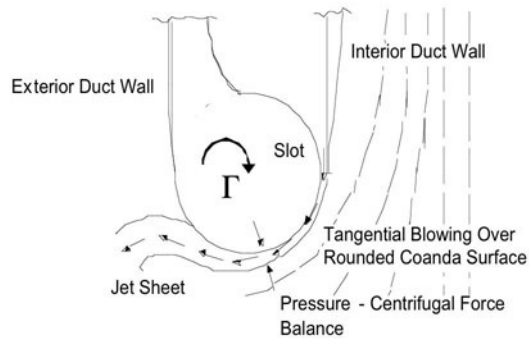
Investigation Objectives

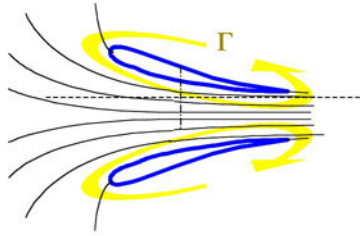
- Investigate the “Morphing Nacelle” concept proposed for the PAV. *This nacelle will employ active pneumatic flow control, as opposed to moving surfaces to optimize off design point operation.*
- Determine what, if any, propulsive performance enhancement can be gained by modifying the circulation about a fan shroud.
- Determine if ground pressure signature can be modified by a “virtual diffuser” effect expected when applying control to the nozzle.

PAV Air TAXI Concept



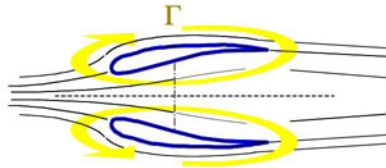
Circulation Control (CC) as Applied to Duct Exit Nozzle



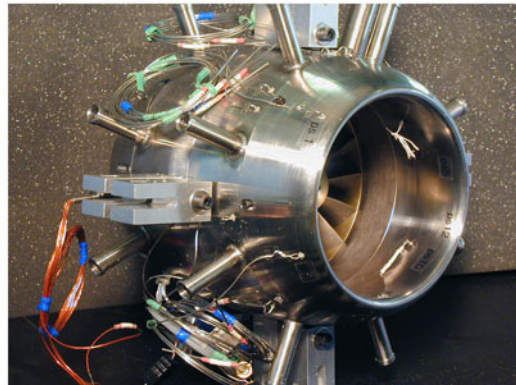


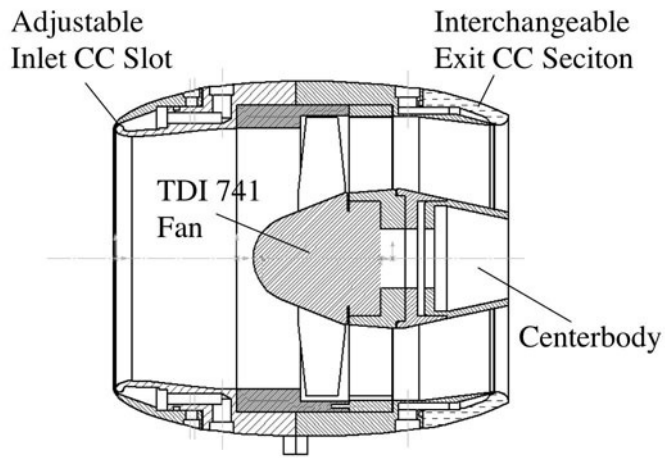
Circulation (Γ)
On a Typical Lifting Fan
(Accelerating Shroud)

Circulation (Γ)
On a Typical Translating Fan
(Decelerating Shroud)

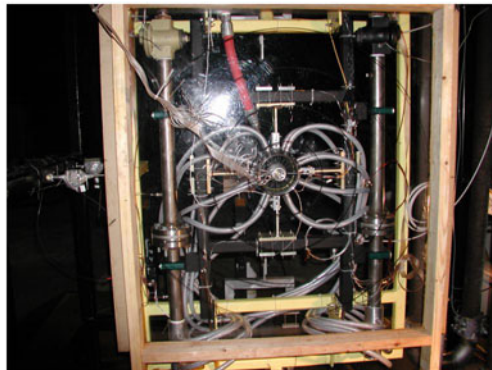


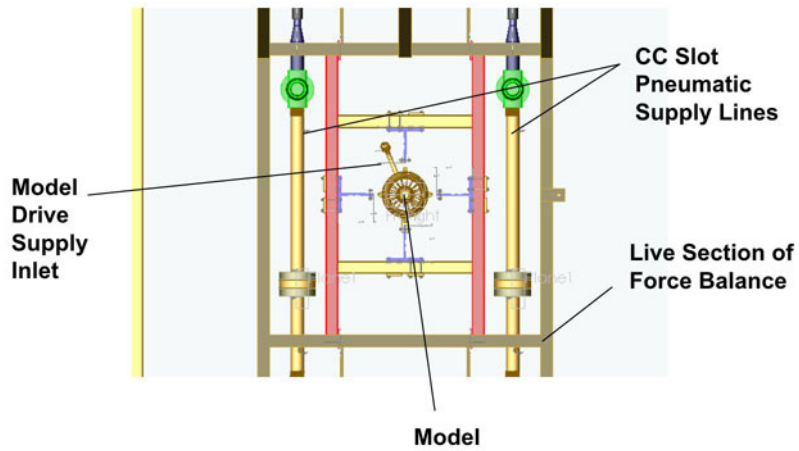
CC Shrouded Fan Model Constructed by M-DOT Aerospace



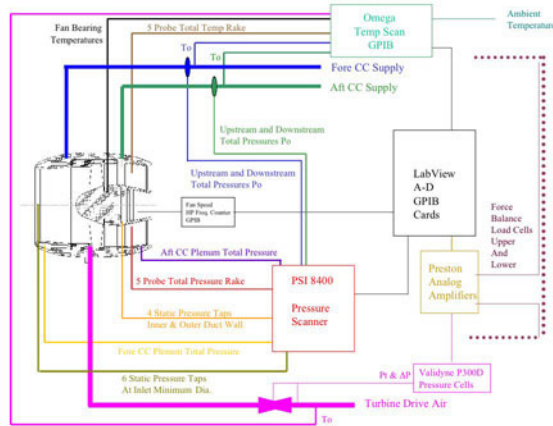


Model Installation in Thrust Cell





Test Instrumentation



Data Reduction

$$C_T = \frac{\text{Thrust}}{\rho_\infty N^2 D^4}$$

N = Fan Rotational Speed
 D = Fan Diameter
 ρ = "Freestream" (ambient) density

$$C_{\mu_s} = \frac{\dot{m}_{jet} V_{jet}}{\rho_\infty N^2 D^4}$$

Assuming an Isentropic Flow
 Expanding to "Freestream Static"
 (i.e. ambient barometric pressure):

C_μ Momentum Coefficient of
 The CC jet, Normally Relates
 Fraction Of Freestream Momentum
 Employed in the Jet

$$V_j = \sqrt{2RT_d \left(\frac{\gamma}{\gamma-1} \right) \left[1 - \frac{P_\infty}{P_d} \right]^{\frac{\gamma-1}{\gamma}}}$$

Data Reduction - Pressures

$$PR = \frac{P_{T_{FAN}}}{P_\infty}$$

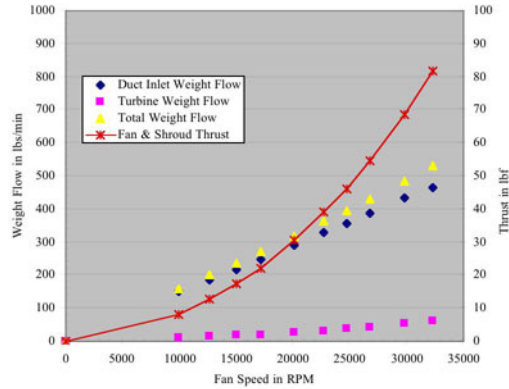
$P_{T_{FAN}}$ Sampled in the
 Middle of Flow Behind the
 Fan Stators

With no freestream dynamic pressure.....

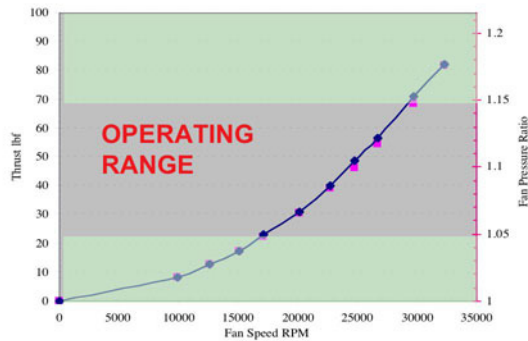
$$C'_p = \frac{P_s - P_\infty}{P_{T_{FAN}}}$$

Relates Fraction of Fan Total
 Pressure at Ground

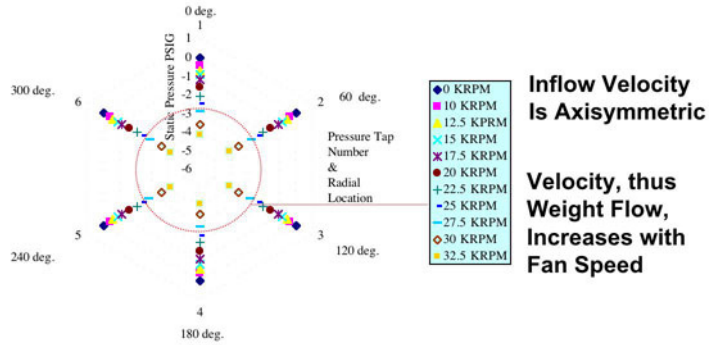
Baseline Shrouded Fan Performance



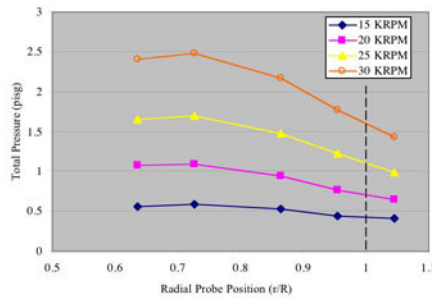
Baseline Fan Thrust Operating Out of Ground Effect



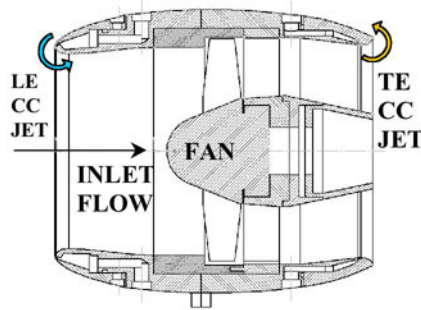
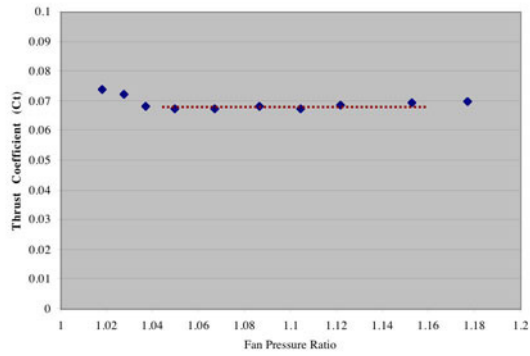
Baseline Inlet Throat Pressure Profile (Circumferential)



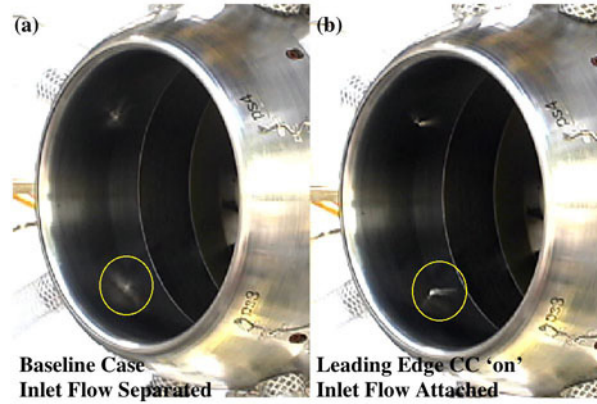
Baseline Total Pressure Profile Behind Fan (in Nozzle)



Baseline Non-Dimensional Performance

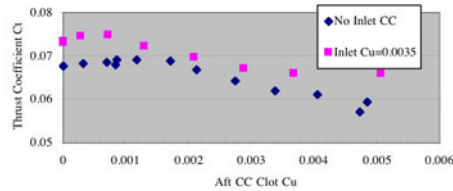


Inlet Stall in Static Operation

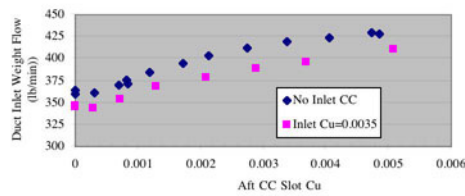


Fan Performance (OGE) with Circulation Control Applied

Static Thrust Performance Varying Nozzle CC Jet Momentum



Corresponding Weight Flow

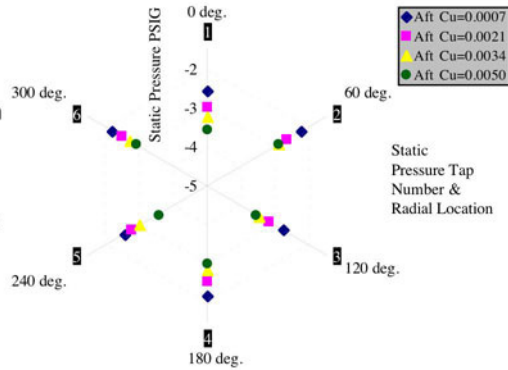


Inlet Static Pressure at Throat Inlet $C_{\mu} = 0.0035$, Nozzle C_m Sweep

Inflow Velocity Increases
With Nozzle CC Momentum

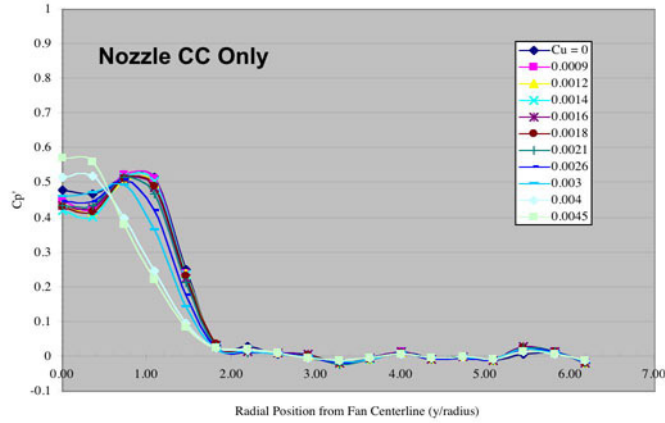
Mean Pressure is Lower
Than Corresponding
Operation Without Inlet CC

Cross Talk Between
Inlet CC Jet
Throat Static Taps

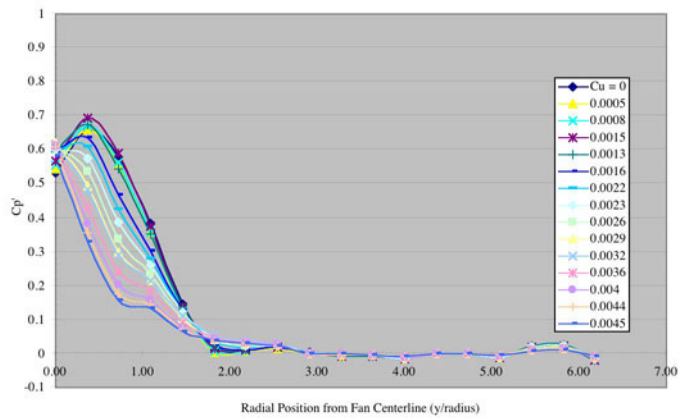


QuickTime Movie

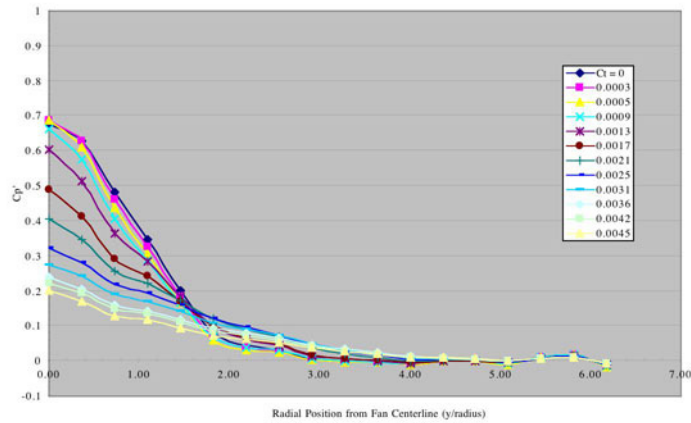
Ground Plane Pressure Signature @ H=1.5 Dia.



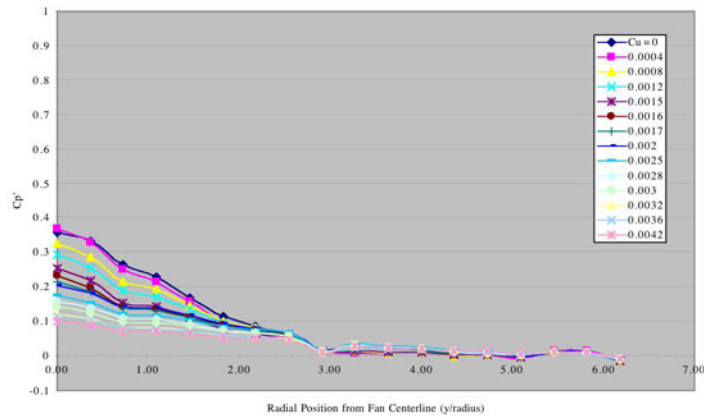
Ground Plane Pressure Signature @ H=3.0 Dia.



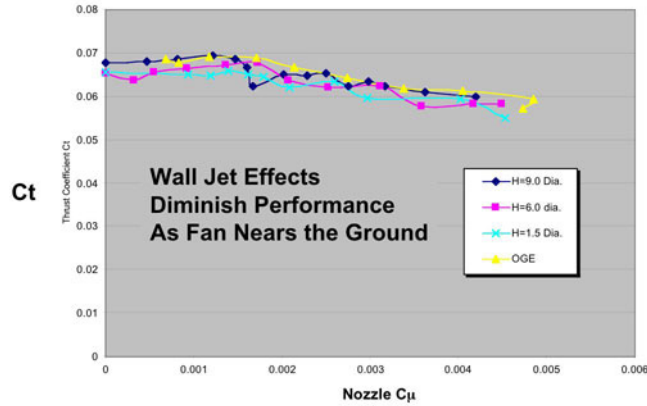
Ground Plane Pressure Signature @ H=6.0 Dia.



Ground Plane Pressure Signature @ H=9.0 Dia.



Comparison of OGE and IGE Performance



Conclusions (1)

- Inlet CC jet blowing can alleviate the stalled inlet condition present in the diffusing duct inlet – which has a positive influence on performance alone.
- Together, the action of CC jets at the duct inlet and nozzle exit can enhance the static thrust of the shrouded fan model at small values of C_{μ_s} ; however, the benefit is lost as C_{μ_s} increases.
- A limited performance enhancement is realized using the nozzle CC device; the observed thrust loss requires additional investigation.

Conclusions (2)

- Some effectiveness if demonstrated in reducing ground plane pressure; however, the interaction between the shroud and ground needs more study.
- The combined operation of inlet and nozzle CC devices must be revisited with improved instrumentation.

Recommendations (1)

- Parametric study of jet slot height effects.
- Parametric study of Coanda (turning surface) shape, especially turning angle.
- In Ground Effect (IGE) operation with a skew angle to the ground plane.
- Revised study of inlet CC jet effects, including a new method to measure inlet weight flow.

Recommendations (2)

- A CFD simulation, calibrated with the model results, for parametric analysis of shroud and CC design variables.
- Detailed flow diagnostics aimed at uncovering the flow physics underlying the CC jet interaction with the fan's flow field.

Acknowledgements

The experimental study described in this paper was supported by NASA Langley Research Center under contract number NAG-1-02093.

The authors wish to acknowledge the following individuals and organizations:

Frank Holman, Bryan Seegers, Hugh Spilsbury, and Scott Ashley of M-DOT Aerospace, for the design, manufacture and construction of the model.

Sandy Shapery, of Shapery Gyronautics, for providing partial financial support for the fabrication of the model and lease of the fan core.